Chem Rev Lett 9 (2026) 732-751

Research Article

Chemical Review and Letters
journal homepage: www.chemrevlett.com
ISSN (online): 2645-4947 (print) 2676-7279

Comprehensive computational investigation of *Aerva lanata* phytoconstituents as potential HER2 kinase inhibitors for the treatment of cancer

Ramenani Hari Babu[1], E. Joel Mart[2], Poonam Dev[3], Varikalla Rajashakar[4], Rubeeya Lodhi[5], Venkateswararao Rachumallu[6], Rajesh Kumar Sharma[7], Varsha Raj[8,*]

[1] *Amity Institute of Pharmacy, Amity University, Gwalior, Madhya Pradesh, India.*
[2]*Department of Pharmacology, Vels Institute of Science, Technology & Advanced Studies (VISTAS), PV Vaithiyalingam Rd, Velan Nagar, Krishnapuram, Pallavaram, Chennai, Tamil Nadu, India.*
[3]*Department of Zoology, St. Ann's College for Women, Mehdipatnam, Hyderabad, Telangana, India.*
[4]*Department of Pharmaceutical Chemistry, Anurag Pharmacy College, Ananthagiri, Surya pet, Telangana, India.*
[5]*Chaitanya Deemed to be University, Chilkur Balaji Temple Road, Himayatnagar, Telangana, India.*
[6]*Department of Data Management, PRA India Pvt Ltd, Chennai, Tamil Nadu, India.*
[7]*Department of Pharmacognosy, Teerthanker Mahaveer College of Pharmacy, Teerthanker Mahaveer University, Delhi Road, Moradabad, India.*
[8]*Kharvel Subharti College of Pharmacy, Swami Vivekanand Subharti University meerut Uttar pradesh, India.*

ARTICLE INFO

Article history:
Received 05 February 2026
Received in revised form 16 April 2026
Accepted 19 April 2026

Keywords:
Aerva lanata
HER2 kinase
Phytochemicals
Molecular docking
ADMET analysis
Anticancer agents

ABSTRACT

Human epidermal growth factor receptor 2 (HER2) is a clinically significant oncogenic kinase that drives tumor growth, survival, and therapeutic resistance, making it a validated target for anticancer drug discovery. In the present study, an integrated in silico strategy was employed to evaluate phytochemicals from *Aerva lanata* as potential HER2 kinase inhibitors by combining ADMET profiling with molecular docking analysis. Sixteen phytochemical constituents belonging to alkaloids, flavonoids, and phenolic acids were selected based on reported phytochemical evidence, structural diversity, and pharmacological relevance. Physicochemical properties, drug-likeness, and pharmacokinetic parameters were predicted using SwissADME and ADMETlab 3.0, revealing that most alkaloids and aglycone flavonoids complied with Lipinski's rule of five, exhibited molecular weights below 500 Da, optimal lipophilicity (logP ~1–3), and acceptable safety profiles. Molecular docking was performed against the HER2 kinase domain using AutoDock Vina integrated in PyRx, followed by interaction analysis in Discovery Studio. Docking results demonstrated binding energies ranging from −4.5 to −9.9 kcal/mol, with several phytochemicals outperforming the native ligand (−8.9 kcal/mol). Notably, apigenin 7-O-β-D-glucoside showed the strongest affinity (−9.9 kcal/mol), followed by 10-methoxy-canthin-6-one (−9.1 kcal/mol), canthin-6-one (−9.0 kcal/mol), and quercetin (−8.3 kcal/mol). These compounds formed multiple hydrogen bonds (bond lengths ~2.0–2.8 Å) and hydrophobic interactions with key catalytic residues such as MET801, LEU796, ASP863, and VAL734, indicating stable ligand–protein complexes. Overall, this study highlights *Aerva lanata* as a promising source of lead scaffolds for HER2-targeted anticancer therapy and provides a strong computational rationale for further *in vitro* and *in vivo* validation.

1. Introduction

Cancer remains one of the leading causes of morbidity and mortality worldwide, necessitating the continuous discovery of novel and effective therapeutic agents [1–3]. Among the various molecular targets implicated in cancer progression, the human epidermal growth factor receptor 2 (HER2) kinase has gained considerable attention due to its critical role in regulating cell proliferation, survival, differentiation, and metastasis [4–6]. Overexpression or aberrant activation of HER2 is strongly associated with aggressive tumor phenotypes, poor prognosis, and

* Corresponding author E-mail: varsharaj01@gmail.com
https://doi.org/10.22034/crl.2026.578647.1802

therapeutic resistance, particularly in breast and gastric cancers [7]. Although several HER2-targeted therapies are clinically available, their long-term use is often limited by drug resistance, cardiotoxicity, and high treatment costs [8]. These challenges underscore the urgent need to identify safer, cost-effective, and structurally diverse HER2 inhibitors, preferably from natural sources. Medicinal plants have historically served as a rich reservoir of bioactive compounds and continue to inspire modern drug discovery [9]. Natural products are characterized by remarkable chemical diversity, biological compatibility, and evolutionary optimization toward molecular targets. In this context, *Aerva lanata*, a traditionally used medicinal plant, has attracted scientific interest due to its broad spectrum of pharmacological properties, including anti-inflammatory, antioxidant, antimicrobial, hepatoprotective, and anticancer activities [10]. Phytochemical investigations of *A. lanata* have revealed the presence of diverse secondary metabolites such as alkaloids, flavonoids, phenolic acids, and other bioactive constituents, many of which are known to modulate key signaling pathways involved in cancer development and progression [11]. Despite its therapeutic potential, the molecular basis of interaction between *A. lanata* phytoconstituents and oncogenic protein targets such as HER2 remains largely unexplored [11,12]. Advances in computational biology have significantly accelerated early-stage drug discovery by enabling the rapid screening of large compound libraries with reduced cost and time. In silico approaches such as absorption, distribution, metabolism, excretion, and toxicity (ADMET) prediction and molecular docking play a pivotal role in prioritizing drug-like molecules and minimizing late-stage failures. ADMET analysis provides valuable insight into the pharmacokinetic behavior, safety profile, and environmental impact of candidate compounds, while molecular docking elucidates ligand–protein binding affinity, interaction patterns, and structural complementarity within the active site of the target protein [13–15]. The integration of these computational techniques offers a rational and efficient framework for identifying promising lead molecules prior to experimental validation.

In the present study, an integrated in silico strategy was employed to evaluate the potential of selected phytoconstituents of *Aerva lanata* as HER2 kinase inhibitors. A panel of phytochemicals representing major chemical classes reported from plants was systematically screened for drug-likeness and ADMET properties, followed by molecular docking analysis against the HER2 kinase domain.

By correlating pharmacokinetic suitability with binding affinity and interaction profiles, this study aimed to identify promising natural lead compounds capable of modulating HER2 activity. These findings are expected to provide mechanistic insights into the anticancer potential of *A. lanata* phytochemicals and establish a computational foundation for further in vitro and in vivo investigations for the development of novel HER2-targeted anticancer agents.

2. Materials and Methods

2.1. Selection of compounds

The selection of phytochemical compounds for the present investigation was guided by an extensive review of the phytochemical and pharmacological literature on *Aerva lanata*. Previous analytical and experimental studies have consistently reported the presence of a broad spectrum of bioactive secondary metabolites in this plant, including alkaloids, flavonoids, phenolic acids, and related compounds with documented therapeutic relevance [16,17]. To ensure scientific rigor and translational relevance, the compounds were selected based on their reported biological activities, structural diversity, and suitability for computational evaluation. Accordingly, a total of sixteen (16) phytochemicals were shortlisted for in silico assessment. The selected alkaloids included 10-methoxy-canthin-6-one, canthin-6-one, and β-carboline-1-propionic acid [16,17]. The flavonoid group comprised kaempferol, quercetin, isorhamnetin, 4′-hydroxy-3,6,7-trimethoxyflavone, 5-hydroxy-2′,3,5′,6,7-pentamethoxyflavone, and apigenin-7-O-β-D-glucoside. Phenolic acids, such as vanillic acid, syringic acid, and p-hydroxybenzoic acid, along with other reported constituents, including hydroquinone, hydroquinone monobenzyl ether, 2-isopropyl-2,5-dihydrofuran, and feruloyl vanillylamine, were also incorporated into the study.

All shortlisted compounds were subsequently evaluated for drug-likeness and ADMET properties to identify pharmacokinetically acceptable candidates for further study. Compounds that satisfied the ADMET criteria were subjected to molecular docking analysis to explore their binding affinity and interaction patterns with the selected target protein.

The three-dimensional structures of all phytochemicals were retrieved from the PubChem database in SDF format and prepared for computational modeling. The chemical structures of all selected compounds are shown in Figure 1.

2.2. ADMET analysis

The absorption, distribution, metabolism, excretion, and toxicity (ADMET) properties of the selected phytocompounds were evaluated using a systematic in silico workflow to assess their drug-likeness and pharmacokinetic suitability [18]. Initially, the chemical structures of all selected compounds were retrieved from PubChem in the SDF format.

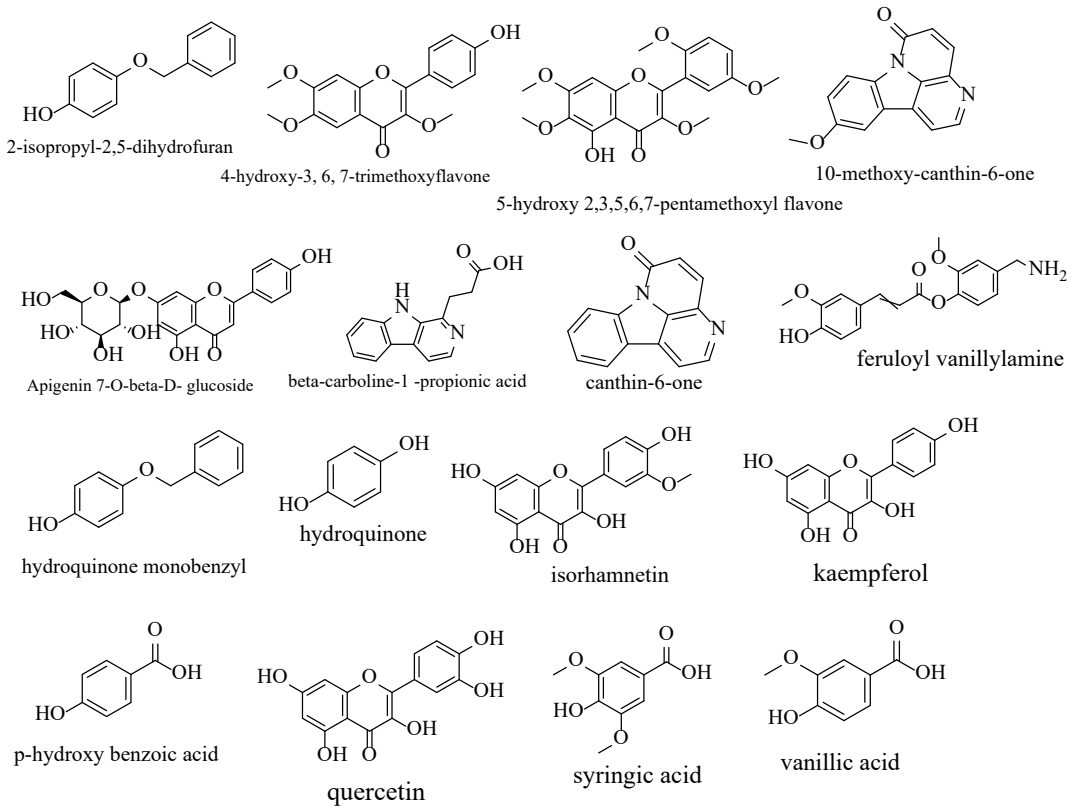

Fig. 1. Chemical Structure of all Selected Compounds.

Where required, the structures were manually drawn and optimized using ChemDraw to ensure correct stereochemistry, valency, and molecular integrity. The finalized structures were converted into SMILES format, which served as the standardized input for subsequent computational analyses. The physicochemical and preliminary pharmacokinetic parameters were predicted using SwissADME. Key descriptors, including molecular weight, lipophilicity (LogP), topological polar surface area (TPSA), number of hydrogen bond donors and acceptors, rotatable bonds, and compliance with Lipinski's rule of five, were analyzed to estimate oral bioavailability and drug-like properties [19–21].

Comprehensive ADMET profiling was performed using ADMETlab 3.0. This platform was employed to predict absorption-related parameters, such as human intestinal absorption and Caco-2 permeability; distribution properties, including plasma protein binding and blood–brain barrier permeability; metabolism characteristics focusing on cytochrome P450 enzyme interactions (CYP inhibition and substrate potential); excretion parameters, such as clearance; and toxicity endpoints, including hepatotoxicity, cardiotoxicity (hERG inhibition), mutagenicity, and carcinogenicity [22]. All predictions were generated using the default model settings. The integrated ADMET evaluation provided a rational basis for prioritizing compounds with favorable pharmacokinetic behaviors and acceptable safety profiles for further molecular docking and biological validation studies.

2.3. Molecular docking analysis

Molecular docking was performed to investigate the binding interactions and affinity of the selected phytocompounds with the target protein. The three-dimensional (3D) structures of the selected ligands were retrieved from PubChem in SDF format. Ligands that were unavailable or required structural correction were drawn manually using ChemDraw, ensuring proper atom types, bond orders, and stereochemistry [23–26]. All ligand structures were subsequently energy-minimized and converted into the appropriate file formats compatible with docking studies. The 3D crystal structure of the target protein was obtained from the Protein Data Bank in PDB format. Protein preparation was carried out using Discovery Studio, which involved removal of crystallographic water molecules, heteroatoms, and co-crystallized ligands, followed by the addition of polar hydrogen atoms and assignment of appropriate partial charges. The prepared protein structure was saved in PDB format for docking. Molecular docking simulations were conducted using PyRx, which integrates AutoDock Vina as the docking engine [27–30]. Ligands were imported in optimized format and converted to PDBQT files prior to docking. The active site of the target protein was defined by setting the grid box parameters based on the known binding pocket, with grid center coordinates set at 13.047658, 1.810132, and 28.168947. Default grid dimensions were maintained to adequately cover the active site region and allow flexible ligand accommodation. Docking was performed using default

exhaustiveness parameters, and multiple binding poses were generated for each ligand. The best docked conformations were selected based on the lowest binding energy (kcal/mol) and favorable interaction profiles. Post-docking analysis, including visualization of hydrogen bonds, hydrophobic interactions, and amino acid residue involvement, was carried out using Discovery Studio.

The docking results provided insights into ligand–protein binding modes and supported the selection of promising compounds for further in vitro antifungal evaluation.3D lines ribbon representation of HER2 kinase with native ligand are shown in Figure 2.

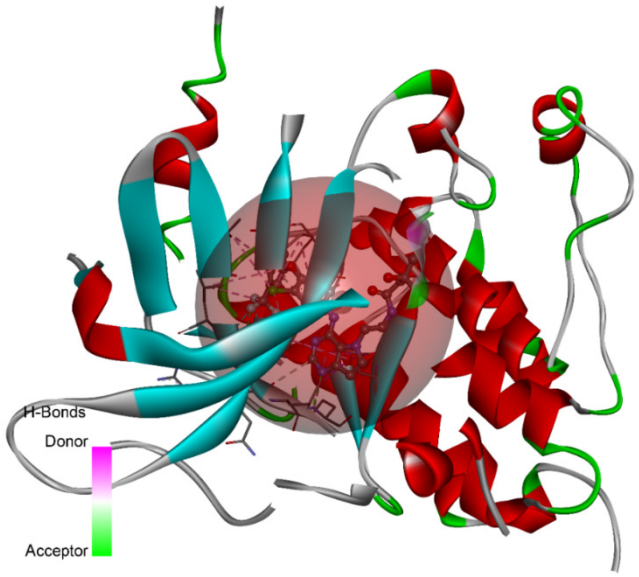

Fig. 2. Three-dimensional (3D) ribbon representation of the HER2 kinase domain in complex with the native ligand. The figure illustrates the overall protein architecture, highlighting the active binding site and spatial orientation of the ligand within the catalytic pocket.

3. Results and Discussion

3.1. ADMET analysis

ADMET analysis plays a crucial role in early-stage drug discovery by predicting the absorption, distribution, metabolism, excretion, and toxicity profiles of candidate molecules, thereby reducing the risk of late-stage drug failure. Evaluating physicochemical properties using in silico ADMET parameters enables the identification of compounds with optimal pharmacokinetic behavior and drug-likeness before experimental validation.

The physicochemical parameters summarized in Table 1 provide critical insights into the structural features governing the pharmacokinetic behavior of the selected compounds. The molecular weight (MW) ranged from 110.04 Da (hydroquinone) to 547.16 Da for the native ligand. Compounds with MW below 500 Da, such as canthin-6-one (220.06 Da) and 10-methoxy-canthin-6-one (250.07 Da), and flavonoids such as kaempferol (286.05 Da) and quercetin (302.04 Da), are generally favorable for oral drug development. In contrast, the native ligand exceeded the recommended MW threshold, which may negatively affect permeability. The topological polar surface area (TPSA) varied considerably, with lower values observed for canthin-6-one (34.37 Å²) and 2-isopropyl-2,5-dihydrofuran (29.46 Å²), suggesting enhanced membrane permeability. Conversely, the high TPSA values for apigenin 7-O-β-D-glucoside (170.05 Å²) and quercetin (131.36 Å²) indicate limited passive diffusion. The LogP values ranged from 0.58 (hydroquinone) to 4.61 (native ligand), with most compounds falling within the optimal lipophilicity window (logP 1–3), supporting balanced solubility and permeability. Overall, Table 1 highlights that alkaloids and aglycone flavonoids possess more favorable physicochemical profiles than glycosylated or bulky derivatives.

The drug-likeness evaluation presented in Table 2 further refines compound prioritization by integrating structural complexity, bioavailability, and medicinal chemistry filters.

The quantitative Estimate of Drug-likeness (QED) values ranged from 0.241 for the native ligand to 0.825 (2-isopropyl-2,5-dihydrofuran and hydroquinone monobenzyl). Higher QED values (>0.6) observed for 4-hydroxy-3,6,7-trimethoxyflavone (0.792), β-carboline-1-propionic acid (0.739), and syringic acid (0.760) indicate a superior overall drug-like quality. All compounds showed zero Lipinski violations, confirming acceptable hydrogen bonding, molecular weight, and lipophilicity. The natural product (NP) scores were positive for most flavonoids (e.g., quercetin 1.701, isorhamnetin 1.566), reflecting their complex yet biologically relevant scaffolds. Some compounds triggered the GSK or Golden Triangle rules, such as native ligands and phenolic acids, suggesting potential challenges in optimization.

Chelator rule alerts observed for flavonoids, such as quercetin and kaempferol, may indicate metal-binding tendencies but do not preclude their therapeutic utility. Collectively, Table 2 supports alkaloids and methoxylated flavones as drug-like leads.

Absorption characteristics predicted in Table 3 reveal substantial variability in intestinal uptake and permeability. Caco-2 permeability values ranged from –4.27 (canthin-6-one) to –6.36 (apigenin 7-O-β-D-glucoside), where less negative values indicate better permeability.

Alkaloids such as canthin-6-one (–4.28) and 10-methoxy-canthin-6-one (–4.54) demonstrated superior epithelial permeability compared to polyphenolic compounds like quercetin (–6.18).

Table 1. Physicochemical and molecular descriptors of selected *Aerva lanata* phytochemicals and the native ligand, including molecular weight, polarity, lipophilicity, solubility, and structural features relevant to drug-likeness.

Compounds	MW	Volume	Dense	nHA	nHD	nRot	nRing	TPSA	logS	logP
Native ligand	547.16	509.7934	1.073297	8	3	11	4	101.3	-6.07271	4.609609
2-isopropyl-2,5-dihydrofuran	200.08	218.053	0.917575	2	1	3	2	29.46	-2.32064	2.901587
4-hydroxy-3, 6, 7-trimethoxyflavone	328.09	325.8645	1.00683	6	1	4	3	78.13	-4.17984	2.132532
5-hydroxy 2,3,5,6,7-pentamethoxyl flavone	388.12	378.0369	1.026672	8	1	6	3	96.59	-3.53102	2.338866
10-methoxy-canthin-6-one	250.07	252.2527	0.991347	4	0	1	4	43.6	-3.60951	2.311253
Apigenin 7-O-β-D-glucoside	432.11	404.3569	1.068635	10	6	4	4	170.05	-3.5185	1.212905
β-carboline-1-propionic acid	240.09	246.1496	0.975382	4	2	3	3	65.98	-3.2497	2.057825
canthin-6-one	220.06	226.1665	0.973	3	0	0	4	34.37	-2.57576	2.043489
feruloyl vanillylamine	329.13	336.6275	0.977728	6	3	7	2	91.01	-2.58051	1.999636
hydroquinone monobenzyl	200.08	218.053	0.917575	2	1	3	2	29.46	-2.32064	2.901587
hydroquinone	110.04	113.447	0.969968	2	2	0	1	40.46	-0.58178	0.589621
isorhamnetin	316.06	300.0628	1.053313	7	4	2	3	120.36	-3.9147	1.824764
kaempferol	286.05	273.9766	1.044067	6	4	1	3	111.13	-3.64796	1.965317
p-hydroxy benzoic acid	138.03	136.8967	1.008278	3	2	1	1	57.53	-1.77037	1.401931
quercetin	302.04	282.7668	1.068159	7	5	1	3	131.36	-3.72159	1.447712
syringic acid	198.05	189.0692	1.0475	5	2	3	1	75.99	-2.1659	1.209245
vanillic acid	168.04	162.983	1.031028	4	2	2	1	66.76	-1.92439	1.339687

Table 2. Drug-likeness assessment of selected *Aerva lanata* phytoconstituents and the native ligand based on quantitative estimate of drug-likeness (QED), natural product score, and major medicinal chemistry filters.

Compounds	QED	NP Score	Lipinski rule	Pfizer Rule	GSK Rule	GoldenTriangle	Chelator Rule
Native ligand	0.241	-1.172	0	0	1	1	0
2-isopropyl-2,5-dihydrofuran	0.825	-0.189	0	0	0	0	0
4-hydroxy-3, 6, 7-trimethoxyflavone	0.792	0.775	0	0	0	0	0
5-hydroxy 2,3,5,6,7-pentamethoxyl flavone	0.688	1	0	0	0	0	1
10-methoxy-canthin-6-one	0.521	0.106	0	0	0	0	0
Apigenin 7-O-β-D-glucoside	0.331	1.934	0	0	1	0	0
β-carboline-1-propionic acid	0.739	0.518	0	0	0	0	0
canthin-6-one	0.456	0.198	0	0	0	0	0
feruloyl vanillylamine	0.481	0.466	0	0	0	0	1
hydroquinone monobenzyl	0.825	-0.189	0	0	0	0	0
hydroquinone	0.491	0.593	0	0	0	1	0
isorhamnetin	0.572	1.566	0	0	0	0	1
kaempferol	0.546	1.546	0	0	0	0	1
p-hydroxy benzoic acid	0.61	0.377	0	0	0	1	0
quercetin	0.434	1.701	0	0	0	0	1
syringic acid	0.76	0.544	0	0	0	1	1
vanillic acid	0.693	0.524	0	0	0	1	1

Table 3. Predicted absorption-related pharmacokinetic parameters of selected phytochemicals, including intestinal permeability, P-glycoprotein interaction, human intestinal absorption, and fraction absorbed at different thresholds.

Compounds	Caco-2 Permeability	MDCK Permeability	Pgp-inhibitor	Pgp-substrate	HIA	F20%	F30%	F50%
Native ligand	-5.23574	-5.08469	0.266528	0.636519	0.022941	0.371214	0.020962	0.997232
2-isopropyl-2,5-dihydrofuran	-4.8342	-4.59881	0.023638	0.008309	0.021864	0.291599	0.169263	0.178151
4-hydroxy-3, 6, 7-trimethoxyflavone	-4.85315	-4.6775	0.890109	0.085763	0.040114	0.094549	0.118408	0.937837
5-hydroxy 2,3,5,6,7-pentamethoxyl flavone	-4.95844	-4.66833	0.992943	0.158241	0.407112	0.04198	0.20149	0.979213
10-methoxy-canthin-6-one	-4.53792	-4.35778	0.558963	0.130556	0.112444	0.180526	0.139237	0.448649
Apigenin 7-O-β-D-glucoside	-6.36043	-5.01883	0.000176	0.391179	0.465437	0.368747	0.990034	0.993549
β-carboline-1-propionic acid	-5.24591	-4.62196	8.84E-05	0.008667	0.006841	0.004715	0.012247	0.019467
canthin-6-one	-4.2756	-4.43019	0.583772	0.112732	0.004519	0.056701	0.143021	0.287049
feruloyl vanillylamine	-5.62165	-4.9781	0.186403	0.082906	0.202332	0.663047	0.557621	0.953882
hydroquinone monobenzyl	-4.8342	-4.59881	0.023638	0.008309	0.021864	0.291599	0.169263	0.178151
hydroquinone	-5.07778	-4.73985	0.018239	0.014532	0.001686	0.364151	0.286354	0.703875
isorhamnetin	-5.48423	-4.86797	0.789891	0.095298	0.119377	0.049905	0.838213	0.992375
kaempferol	-5.96934	-4.90902	0.14215	0.163041	0.015143	0.084482	0.715565	0.983332
p-hydroxy benzoic acid	-5.11051	-4.79538	0.001654	0.280958	0.097897	0.319174	0.169181	0.715748
quercetin	-6.17681	-4.92272	0.027569	0.030731	0.133589	0.503898	0.99108	0.998593
syringic acid	-5.19884	-4.78484	0.616712	0.333231	0.040125	0.087448	0.025154	0.362649
vanillic acid	-5.09626	-4.77351	0.004502	0.217586	0.11145	0.155723	0.054823	0.560547

Human intestinal absorption (HIA) probabilities were generally low to moderate; however, 5-hydroxy-2,3,5,6,7-pentamethoxyflavone (0.407) and apigenin glycoside (0.465) showed relatively higher absorption potential. Many compounds were predicted as P-glycoprotein substrates, such as native ligand (0.64) and quercetin (0.03), which may reduce intracellular accumulation due to efflux. Fraction absorbed values (F20%, F30%, F50%) highlighted that several compounds reach meaningful absorption at higher thresholds, particularly quercetin (F50% = 0.998) and isorhamnetin (0.992). Overall, Table 3 indicates alkaloids possess better intrinsic permeability, while flavonoids may require formulation strategies to enhance absorption.

The distribution and metabolic predictions summarized in Table 4 indicate extensive plasma protein binding (PPB) for most compounds, with values exceeding 95% for the native ligand (99.09%), quercetin (98.66%), and isorhamnetin (98.34%). High PPB may prolong circulation time but reduce free drug concentration.

The volume of distribution (VD) values were generally low to moderate, suggesting confinement mainly within the plasma and extracellular fluids. Blood–brain barrier (BBB) penetration is limited for most flavonoids (e.g., quercetin 0.0004, kaempferol 0.001), indicating minimal central nervous system (CNS) exposure. In contrast, canthin-6-one (0.38) showed relatively higher BBB permeability, which may be advantageous or undesirable depending on the therapeutic targets. CYP450 interaction analysis revealed that many compounds act as substrates rather than inhibitors, particularly CYP3A4, reducing the likelihood of adverse drug–drug interactions. Alkaloids showed broader CYP involvement, whereas glycosides exhibited minimal metabolic interactions. Thus, Table 4 supports the favorable metabolic safety of most compounds, especially flavonoids.

Table 4. In silico distribution and metabolism profiles of selected *Aerva lanata* phytochemicals, highlighting plasma protein binding, volume of distribution, blood–brain barrier permeability, and cytochrome P450 interactions.

Compounds	Distribution				Metabolism									
	PPB %	VD	BBB	Fu	CYP1A2		CYP2C19		CYP2C9		CYP2D6		CYP3A4	
					Inhibitor	Substrate	Inhibitor	Substrate	Inhibitor	Substrate	Inhibitor	Substrate	Inhibitor	Substrate
Native ligand	99.09294	0.273474	0.154844	0.429866	0.02057	0.393111	0.036818	0.007027	0.0195	0.000168	6.53E-05	0.000225	0.114765	0.999905
2-isopropyl-2,5-dihydrofuran	97.6864	0.267119	0.277744	1.807737	0.993152	0.412608	0.980856	0.301373	0.067139	0.921746	0.030971	0.999431	0.06112	0.128935
4-hydroxy-3, 6, 7-trimethoxyflavone	94.87235	-0.08133	0.002382	4.406625	0.030282	0.964375	0.250276	0.996066	0.181777	0.271697	0.000396	0.504925	0.921031	0.966719
5-hydroxy 2,3,5,6,7-pentamethoxyl flavone	85.85183	-0.48336	0.012763	10.0254	0.984038	0.998198	0.558509	0.734662	0.277982	0.896032	0.001719	0.902334	0.697579	0.049286
10-methoxy-canthin-6-one	87.41169	-0.02828	0.038148	12.23605	0.999988	0.99929	0.706802	0.99589	0.716327	0.999335	0.448664	0.989505	0.956959	0.129448
Apigenin 7-O-β-D-glucoside	83.75095	-0.04714	0.003549	14.27875	0.001123	4.77E-05	6.85E-06	9.91E-07	6.06E-06	0.000229	0.000172	0.000952	0.037287	8.43E-07
β-carboline-1-propionic acid	97.20608	-0.75507	0.011929	1.449869	0.000361	0.002908	1.44E-08	0.570698	2.26E-08	0.999882	0.000375	0.000346	2.42E-06	0.037499
canthin-6-one	94.75171	-0.0795	0.384498	6.318909	1	0.998477	0.635762	0.630448	0.946031	0.955838	0.786769	0.825791	0.651809	0.711474
feruloyl vanillylamine	63.37863	0.068624	0.021597	38.27625	0.073863	0.643635	0.001384	0.99211	2.00E-05	0.991773	0.000698	0.09228	0.001173	8.89E-05
hydroquinone monobenzyl	97.6864	0.267119	0.277744	1.807737	0.993152	0.412608	0.980856	0.301373	0.067139	0.921746	0.030971	0.999431	0.06112	0.128935
hydroquinone	24.16628	-0.02819	0.025911	68.32486	0.789206	0.042139	0.038417	0.038367	0.059116	0.367889	0.11763	0.990192	0.085296	0.065149
isorhamnetin	98.33522	-0.78444	0.000106	1.150948	0.999643	0.850024	0.178334	0.00563	0.875218	0.186766	0.007985	0.998295	0.976015	9.74E-05
kaempferol	97.88079	-0.81165	0.000951	1.360188	0.996672	0.598314	0.132402	0.000515	0.799358	0.518549	0.00489	0.994622	0.974528	0.001706
p-hydroxy benzoic acid	75.92269	-0.61282	0.005552	19.9651	0.002003	0.000742	0.000119	0.005616	0.004069	0.25038	0.000231	0.016	0.000724	0.003851
quercetin	98.65997	-0.87913	0.000445	1.131221	0.998312	0.38429	0.005855	4.87E-05	0.432249	0.029644	0.00018	0.978297	0.936699	1.34E-06
syringic acid	76.52587	-0.63096	0.216208	18.66545	0.000455	0.020249	0.010511	0.040752	0.003657	0.106528	0.007765	0.001338	0.005643	0.001208
vanillic acid	67.70231	-0.67118	0.002189	25.95035	0.001958	0.015754	0.002598	0.029476	0.000776	0.093576	0.016766	0.014894	0.002813	0.001667

The excretion and toxicity predictions in Table 5 demonstrate acceptable elimination and safety profiles for most compounds.

The plasma clearance (CL-plasma) values ranged from 3.04 (vanillic acid) to 17.04 (hydroquinone), indicating moderate elimination rates. Half-life values were generally between 0.5–2.5 h, supporting manageable systemic exposure. The toxicity endpoints predominantly indicated a low to moderate risk. The Ames toxicity probabilities were below the critical concern for most compounds, with kaempferol (0.545) and quercetin (0.586) indicating non-mutagenic tendencies. Hepatotoxicity (H-HT) and DILI predictions were higher for the native ligands, suggesting caution, whereas phenolic acids and flavonoids showed safer profiles. The skin sensitization and carcinogenicity probabilities were low for most natural compounds. Overall, Table 5 confirms that the traditionally used phytochemicals possess acceptable safety margins, reinforcing their suitability for further development.

Table 5. Predicted excretion characteristics and toxicity endpoints of selected phytoconstituents and the native ligand, including clearance, half-life, organ toxicity, mutagenicity, and safety-related parameters.

Compounds	Excretion	Toxicity										
	CL-plasma	T1/2	H-HT	DILI	Ames Toxicity	Rat Oral Acute Toxicity	FDAMDD	Skin Sensitization	Carcinogenicity	Eye Corrosion	Eye Irritation	Respiratory Toxicity
Native ligand	5.959764	0.545126	0.894356	0.97583	0.583268	0.370041	0.670105	0.362738	0.361974	1.09E-07	0.091755	0.868925
2-isopropyl-2,5-dihydrofuran	11.91061	0.913361	0.198199	0.194639	0.34528	0.119305	0.370093	0.642519	0.603508	0.316748	0.986053	0.474276
4-hydroxy-3, 6, 7-trimethoxyflavone	8.891344	1.601924	0.437677	0.659584	0.443422	0.421149	0.645222	0.461507	0.809457	0.451027	0.974979	0.564692
5-hydroxy 2,3,5,6,7-pentamethoxyl flavone	5.924212	1.044578	0.482783	0.85418	0.540909	0.344794	0.474224	0.319027	0.863711	0.23398	0.91782	0.674075
10-methoxy-canthin-6-one	8.171058	0.881733	0.780004	0.937986	0.934656	0.621253	0.81176	0.042859	0.906588	4.17E-05	0.42568	0.928665
Apigenin 7-O-β-D-glucoside	3.213789	3.454334	0.6376	0.977205	0.909948	0.047003	0.106948	0.989233	0.471574	2.91E-05	0.631624	0.035892
β-carboline-1-propionic acid	4.964782	1.097351	0.618945	0.792492	0.561638	0.467002	0.504444	0.206591	0.572373	0.00226	0.960174	0.883919
canthin-6-one	7.449738	1.15858	0.756695	0.805824	0.894929	0.564713	0.653889	0.257579	0.851968	0.001806	0.737909	0.870409
feruloyl vanillylamine	7.045929	0.997765	0.315047	0.069232	0.440689	0.614679	0.682036	0.998435	0.117754	0.966318	0.752129	0.928669
hydroquinone monobenzyl	11.91061	0.913361	0.198199	0.194639	0.34528	0.119305	0.370093	0.642519	0.603508	0.316748	0.986053	0.474276
hydroquinone	17.04294	1.765023	0.392161	0.182502	0.518454	0.553223	0.489591	0.987261	0.750009	0.991065	0.998274	0.665768
isorhamnetin	3.857877	1.703521	0.383415	0.724618	0.598837	0.482418	0.740455	0.670375	0.681567	0.554961	0.997021	0.796159
kaempferol	5.694431	1.38759	0.386179	0.702867	0.545969	0.487835	0.804589	0.621322	0.715984	0.575216	0.998204	0.712718
p-hydroxy benzoic acid	3.456142	1.667961	0.424388	0.363316	0.275301	0.24811	0.133938	0.413493	0.427906	0.859868	0.998417	0.550761
quercetin	8.288988	1.58575	0.337382	0.782596	0.586042	0.479917	0.788757	0.896924	0.600177	0.603284	0.998417	0.673657
syringic acid	3.223177	2.455797	0.484285	0.650168	0.32158	0.322106	0.119834	0.477641	0.415719	0.806909	0.99046	0.702334
vanillic acid	3.040032	1.977672	0.466211	0.519442	0.383583	0.249182	0.122744	0.548072	0.413194	0.822958	0.995716	0.672326

The environmental toxicity assessment in Table 6 revealed a generally low ecological risk for most compounds. The bioconcentration factor (BCF) values were below 2 for all molecules, indicating limited bioaccumulation potential.

Lower BCF values were observed for β-carboline-1-propionic acid (0.19) and syringic acid (0.25), suggesting their environmental safety. Aquatic toxicity parameters (IGC50, LC50FM, LC50DM) showed moderate values across compounds, with glycosylated and phenolic acids exhibiting lower toxicity than lipophilic alkaloids. For instance, apigenin 7-O-β-D-glucoside exhibited a lower IGC50 (2.98) than canthin-6-one (4.17). These results indicate that most compounds are environmentally benign and are unlikely to pose ecological hazards during pharmaceutical development.

The ADMET radar summary illustrating the comparative pharmacokinetic and drug-likeness profiles of the most potent *Aerva lanata* phytochemicals and the native ligand are shown in Table 7.

Table 6. Environmental toxicity assessment of selected phytochemicals based on bioconcentration factor and aquatic toxicity indices, indicating potential ecological impact.

Compounds	BCF	IGC50	LC50FM	LC50DM
Native ligand	1.415082	3.764566	4.870027	5.500089
2-isopropyl-2,5-dihydrofuran	1.447951	4.223595	4.528766	4.746445
4-hydroxy-3, 6, 7-trimethoxyflavone	1.114949	3.723172	4.078883	4.380126
5-hydroxy 2,3,5,6,7-pentamethoxyl flavone	1.448176	3.734289	4.088157	4.747932
10-methoxy-canthin-6-one	1.481177	4.01244	4.78199	5.093218
Apigenin 7-O-β-D-glucoside	0.475118	2.976902	3.564616	4.313864
β-carboline-1-propionic acid	0.19088	2.866782	3.334685	4.025209
canthin-6-one	1.481247	4.170472	4.880582	5.003637
feruloyl vanillylamine	0.607304	3.428797	3.9461	4.370366
hydroquinone monobenzyl	1.447951	4.223595	4.528766	4.746445
hydroquinone	1.369493	3.500777	3.949962	4.386039
isorhamnetin	1.098311	3.560594	3.771446	4.302098
kaempferol	1.241837	3.653071	4.00664	4.37644
p-hydroxy benzoic acid	0.611482	2.436611	3.110776	3.72847
quercetin	1.210035	3.758566	4.112	4.485008
syringic acid	0.255189	2.686035	3.09164	3.675891
vanillic acid	0.379278	2.602067	2.980854	3.670131

Table 7. ADMET radar summary illustrating the comparative pharmacokinetic and drug-likeness profiles of the most potent *Aerva lanata* phytochemicals and the native ligand.

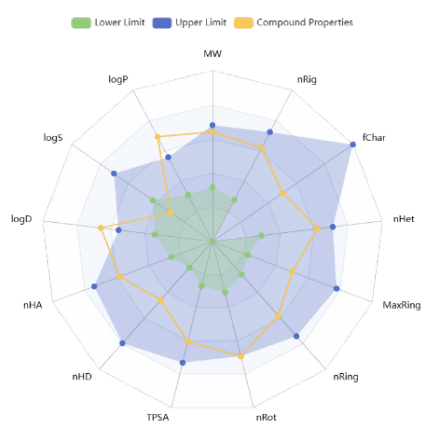	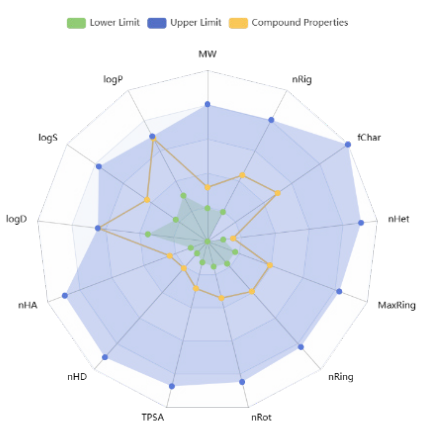	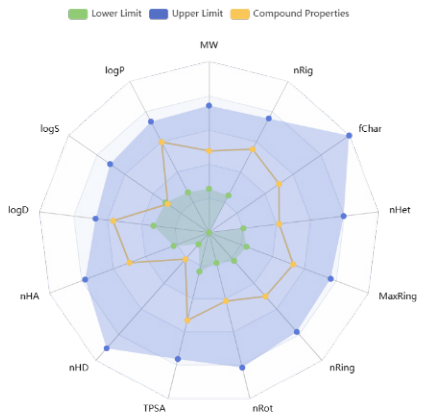
Native Ligand	2-isopropyl-2,5-dihydrofuran	4-hydroxy-3, 6, 7-trimethoxyflavone
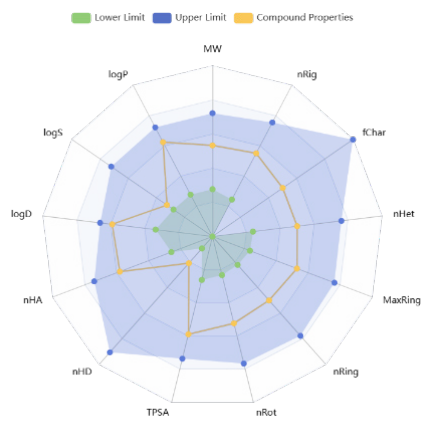	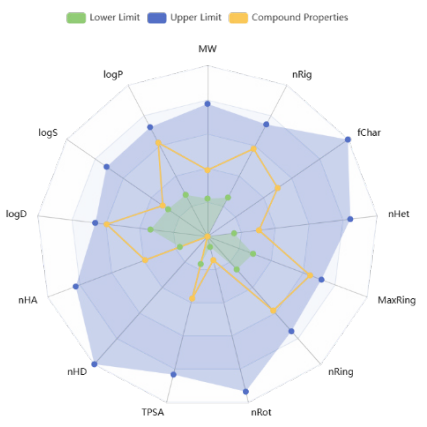	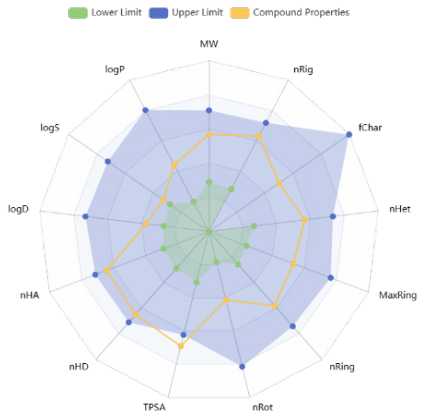
5-hydroxy 2,3,5,6,7-pentamethoxyl flavone	10-methoxy-canthin-6-one	Apigenin 7-O-β-D-glucoside

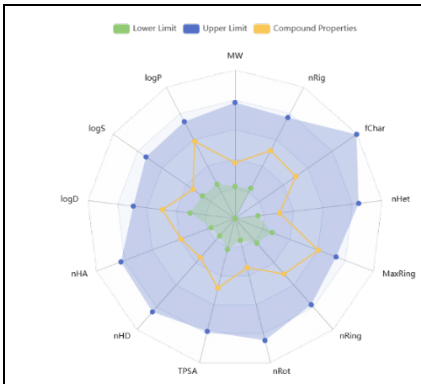	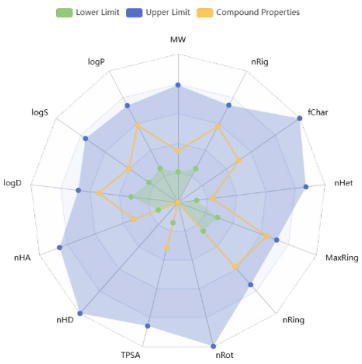	
β-carboline-1-propionic acid	canthin-6-one	feruloyl vanillylamine
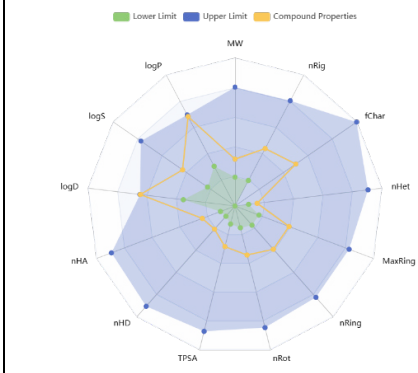	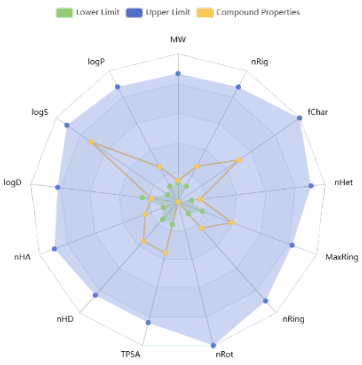	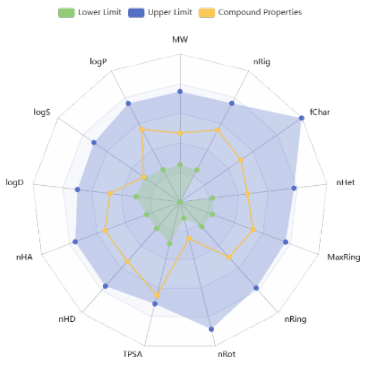
hydroquinone monobenzyl	hydroquinone	isorhamnetin
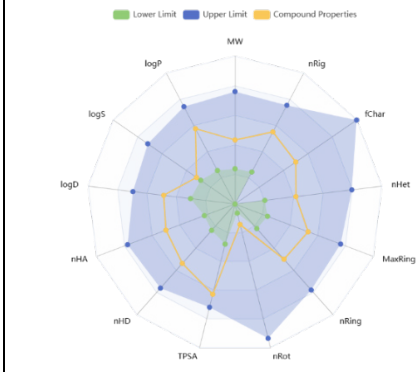	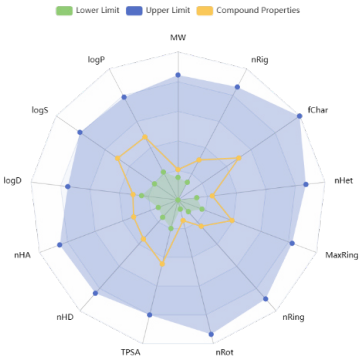	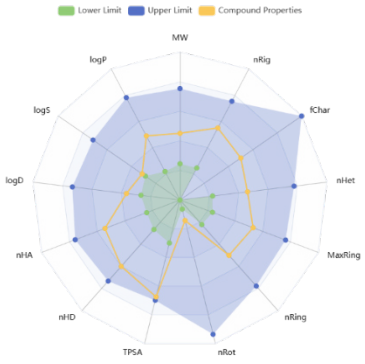
kaempferol	p-hydroxy benzoic acid	quercetin
	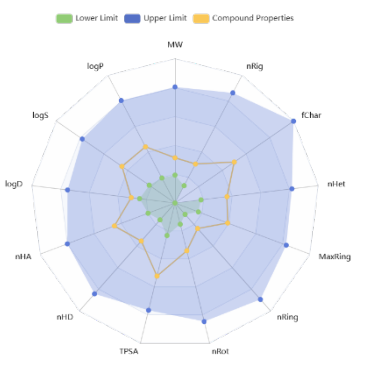	
syringic acid	vanillic acid	

3.2. Molecular docking

Molecular docking analysis of the selected phytochemicals against the HER2 kinase domain revealed substantial variability in binding affinity, interaction profiles, and binding site complementarity compared with the native ligand (Tables 8 and 9). These differences largely reflect the influence of molecular size, functional group diversity, and aromatic scaffolds on ligand–protein recognition and stabilization within the HER2 active site.

Among all the screened compounds, apigenin 7-O-β-D-glucoside exhibited the strongest binding affinity, with a docking score of −9.9 kcal/mol, outperforming the native ligand (−8.9 kcal/mol).

This superior affinity can be attributed to the extensive hydrogen-bonding network and hydrophobic interactions. Apigenin 7-O-β-D-glucoside formed multiple conventional hydrogen bonds with key catalytic residues LEU796 (2.24 Å), MET801 (2.78 Å), and THR862 (2.03 Å), along with a carbon–hydrogen bond with ASP863. These polar interactions were further stabilized by π–π stacking with PHE1004 and π–σ/π–alkyl interactions with LEU852, LEU726, VAL734, and ALA751, indicating deep and stable anchoring within the HER2 binding pocket.

In contrast, the native ligand formed fewer hydrogen bonds, suggesting a comparatively weaker polar stabilization despite its larger molecular size. Canthin-6-one alkaloids also exhibited excellent binding performance relative to native ligands. 10-Methoxy-canthin-6-one achieved a docking score of −9.1 kcal/mol, slightly exceeding that of the native ligand. It established a strong conventional hydrogen bond with MET801 (2.19 Å) and a carbon hydrogen bond with ASP863, residues that are critical for HER2 kinase inhibition. These interactions were reinforced by extensive hydrophobic contacts with LEU852, VAL734, LEU726, and ALA751, suggesting efficient occupation of the hydrophobic regions of the active site of the enzyme. Similarly, canthin-6-one showed a docking score of −9.0 kcal/mol and formed a stable hydrogen bond with MET801 (2.25 Å), along with multiple π–alkyl interactions, highlighting a binding behavior comparable to or better than that of the native ligand.

The native ligand exhibited a docking score of −8.9 kcal/mol with a relatively high ligand energy (556.84 kcal/mol), indicating a stable but energetically demanding binding native ligand.

It formed a key hydrogen bond with ASP863 (2.17 Å) and additional stabilizing interactions, including halogen bonds with SER783 and LEU785, a carbon hydrogen bond with GLN799, and π–σ, π–π T-shaped, and π–alkyl interactions with LEU785, PHE864, VAL734, ALA751, and LEU796. While these interactions confirm its suitability as a reference ligand, the reduced number of conventional hydrogen bonds compared to top-performing phytochemicals explains its comparatively lower docking scores.

Flavonoids such as quercetin, kaempferol, and isorhamnetin also demonstrated strong and consistent binding patterns within the HER2 active site. Quercetin showed a docking score of −8.3 kcal/mol, forming multiple hydrogen bonds with LEU796, MET801, and LYS753, along with a carbon hydrogen bond with GLY804.

These interactions were further supported by hydrophobic contacts with VAL734 and LEU852, resulting in binding affinity comparable to native ligand. Kaempferol (−8.1 kcal/mol) primarily interacted through a π-donor hydrogen bond with ASP863 and hydrophobic contacts with LEU785, VAL734, and ALA751, while isorhamnetin (−8.0 kcal/mol) formed a conventional hydrogen bond with MET801 and additional stabilizing interactions with GLY804, THR798, VAL734, and LEU852.

Although slightly weaker than the native ligand, these flavonoids retained favorable interaction geometries within the catalytic pocket. Compounds such as β-carboline-1-propionic acid, 4′-hydroxy-3,6,7-trimethoxyflavone, 5-hydroxy-2′,3,5′,6,7-pentamethoxyflavone, feruloyl vanillylamine, and 2-isopropyl-2,5-dihydrofuran exhibited moderate docking scores (−7.2 to −7.9 kcal/mol). These ligands typically formed one or two hydrogen bonds with residues such as ASP863, LYS753, SER783, or THR798, accompanied by limited hydrophobic interactions, resulting in less stable complexes compared to native ligand. In contrast, small phenolic acids and simple molecules, including syringic acid, vanillic acid, p-hydroxybenzoic acid, and hydroquinone, displayed weak binding affinities (−4.5 to −6.1 kcal/mol).

Their limited interaction capacity and reduced hydrophobic surface area hindered effective engagement with the HER2 binding pocket, making them substantially inferior to the native ligand. Overall, comparative docking analysis clearly demonstrates that several phytochemicals—particularly apigenin 7-O-β-D-glucoside, 10-methoxy-canthin-6-one, canthin-6-one, and quercetin—exhibited equal or superior binding affinity and interaction networks compared to the native ligand.

These compounds achieved stronger or comparable docking scores through a synergistic combination of hydrogen bonding, π-interactions, and hydrophobic contacts with key catalytic residues. Collectively, these findings highlight flavonoids and canthin-6-one alkaloids as promising lead scaffolds for further experimental validation and development of novel HER2-targeted anticancer agents.

Table 8. Two-dimensional (2D) and three-dimensional (3D) binding interaction representations of selected phytochemicals and the native ligand within the HER2 kinase active site. The interactions include hydrogen bonds, hydrophobic contacts, and π-interactions with key amino acid residues, demonstrating ligand–protein binding patterns and stability.

Amino Acid	Bond Length	Bond Type	Bond Category	Ligand Energy (Kcal/mol)	Docking Score
Native ligand					
ASP863	2.17664	Hydrogen Bond	Conventional Hydrogen Bond	556.84	-8.9
LEU785	2.94423	Hydrogen Bond;Halogen	Conventional Hydrogen Bond;Halogen (Fluorine)		
GLN799	3.76598	Hydrogen Bond	Carbon Hydrogen Bond		
SER783	2.74741	Halogen	Halogen (Fluorine)		
SER783	3.21657				
SER783	3.49067				
ARG784	3.56247				
LEU785	3.88839	Hydrophobic	Pi-Sigma		
PHE864	5.43529		Pi-Pi T-shaped		
LEU800	5.43255		Alkyl		
LEU852	4.47961				
LYS753	4.66397				
LEU796	5.07294				
LEU785	4.38106				
ALA751	4.80879				
VAL734	5.28713		Pi-Alkyl		
ALA751	5.13896				
LYS753	4.18287				
LEU796	4.96499				
PHE864	4.91668				
2-isopropyl-2,5-dihydrofuran					
SER783	2.2551	Hydrogen Bond	Conventional Hydrogen Bond	112.93	-7.2
LYS753	3.65351	Hydrophobic	Pi-Sigma		
LEU785	3.39826				
VAL734	5.08697		Pi-Alkyl		
ALA751	4.71746				
4'-hydroxy-3,6,7-trimethoxyflavone					
LYS753	2.06819	Hydrogen Bond	Conventional Hydrogen Bond	419.28	-7.9
ASP863	3.59624		Carbon Hydrogen Bond		
ASP863	3.71508				
LEU852	3.5113	Hydrophobic	Pi-Sigma		
VAL734	4.77119		Pi-Alkyl		
ALA751	4.99803				
LYS753	4.58896				
ALA751	4.36984				
5-hydroxy_2',3,5',6,7-pentamethoxyl_flavone					
THR798	3.44689	Hydrogen Bond	Carbon Hydrogen Bond	602.72	-7.3
ALA751	3.3088				
LEU796	3.51122				
VAL734	5.0294	Hydrophobic	Pi-Alkyl		
ALA751	5.38648				
LYS753	4.91772				
VAL734	4.98443				
LEU852	4.99054				
LYS753	4.91203				
LEU796	5.22081				
10-methoxy-canthin-6-one					
MET801	2.19111	Hydrogen Bond	Conventional Hydrogen Bond	449.67	-9.1
ASP863	3.49465		Carbon Hydrogen Bond		
LEU852	3.93192	Hydrophobic	Pi-Sigma		
LEU726	5.09887		Pi-Alkyl		
VAL734	4.72846				
LEU852	5.38437				

Amino Acid	Bond Length	Bond Type	Bond Category	Ligand Energy (Kcal/mol)	Docking Score
ALA751	4.67034				
VAL734	4.89786				
LEU852	5.13394				
Apigenin 7-O-β-D-glucoside					
LEU796	2.24905	Hydrogen Bond	Conventional Hydrogen Bond	317.37	-9.9
MET801	2.78375				
THR862	2.03246				
ASP863	3.66369		Carbon Hydrogen Bond		
LEU852	3.80011	Hydrophobic	Pi-Sigma		
PHE100 4	3.886		Pi-Pi Stacked		
LEU726	5.15651		Pi-Alkyl		
ALA751	5.45144				
VAL734	4.8531				
LEU852	4.59389				
LEU726	4.91305				
β-carboline-1-propionic acid					
ASP863	2.75671	Hydrogen Bond	Conventional Hydrogen Bond	361.8	-7.6
ALA751	2.32789				
LEU796	2.20343				
LEU852	3.91082	Hydrophobic	Pi-Sigma		
LEU852	3.58086				
VAL734	4.4803		Pi-Alkyl		
LYS753	5.37769				
VAL734	4.92312				
ALA751	4.3858				
canthin-6-one					
MET801	2.25207	Hydrogen Bond	Conventional Hydrogen Bond	437.6	-9
LEU726	3.91637	Hydrophobic	Pi-Sigma		
LEU852	3.49049				
LEU852	3.9599				
VAL734	4.83717		Pi-Alkyl		
LEU852	5.34892				
ALA751	4.60201				
VAL734	4.89774				
ALA751	4.30796				
feruloyl_vanillylamine					
PHE864	2.77955	Hydrogen Bond	Conventional Hydrogen Bond	241.71	-7.4
THR798	3.41117		Carbon Hydrogen Bond		
VAL734	3.88774	Hydrophobic	Pi-Sigma		
ALA751	4.94182		Pi-Alkyl		
LEU852	4.89523				
LEU785	5.43058				
LEU796	4.62626				
Hydroquinone					
ALA751	2.35106	Hydrogen Bond	Conventional Hydrogen Bond	45.69	-4.8
LYS753	2.42835				
hydroquinone_monobenzyl					
LYS753	3.65336	Hydrophobic	Pi-Sigma	112.93	-7.2
LEU785	3.39137				
VAL734	5.05788		Pi-Alkyl		
ALA751	4.71002				
isorhamnetin					
MET801	2.35573	Hydrogen Bond	Conventional Hydrogen Bond	206.32	-8
GLY804	3.40161		Carbon Hydrogen Bond		
VAL734	3.80839	Hydrophobic	Pi-Sigma		
THR798	3.79955				
LEU852	3.48253				
ALA751	4.46776		Pi-Alkyl		

Amino Acid	Bond Length	Bond Type	Bond Category	Ligand Energy (Kcal/mol)	Docking Score
LEU852	4.952				
kaempferol					
ASP863	3.09699	Hydrogen Bond	Pi-Donor Hydrogen Bond	179.69	-8.1
LEU785	3.63153	Hydrophobic	Pi-Sigma		
VAL734	5.11894		Pi-Alkyl		
ALA751	4.20139				
LYS753	5.2089				
p-hydroxy_benzoic_acid					
SER783	2.74756	Hydrogen Bond	Conventional Hydrogen Bond	53.24	-4.5
LEU785	3.78615	Hydrophobic	Pi-Sigma		
PHE864	5.09401		Pi-Pi T-shaped		
LEU796	5.33599		Pi-Alkyl		
Quercetin					
LEU796	2.39886	Hydrogen Bond	Conventional Hydrogen Bond	181.05	-8.3
MET801	2.4944				
LYS753	2.41952				
GLY804	3.45712		Carbon Hydrogen Bond		
VAL734	3.85488	Hydrophobic	Pi-Sigma		
LEU852	3.46938				
LEU852	4.89556		Pi-Alkyl		
syringic_acid					
LEU796	1.79554	Hydrogen Bond	Conventional Hydrogen Bond	110.62	-6.1
SER783	3.28512		Carbon Hydrogen Bond		
THR798	3.6224				
LEU785	5.35678	Hydrophobic	Pi-Alkyl		
LEU796	4.70304				
vanillic_acid					
LEU796	1.93499	Hydrogen Bond	Conventional Hydrogen Bond	81.11	-5.8
ASP863	2.11921				
THR798	3.03644				
SER783	3.40395		Carbon Hydrogen Bond		
LYS753	4.98647	Hydrophobic	Pi-Alkyl		
LEU785	5.37638				
LEU796	4.6355				

Table 9. 2D and 3D binding interaction representations of the most potent phytochemicals and the native ligand within the HER2 kinase active site.

3D Binding Interaction	2D Binding Interaction
Native Ligand	
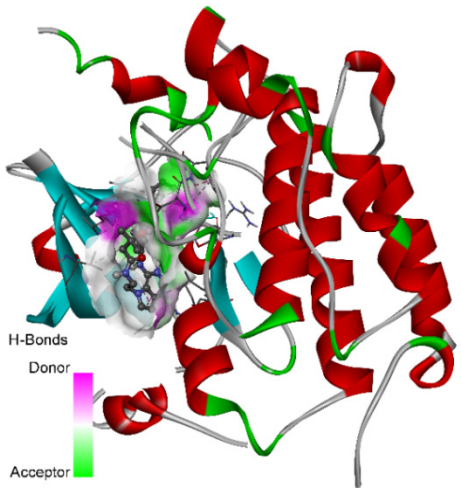	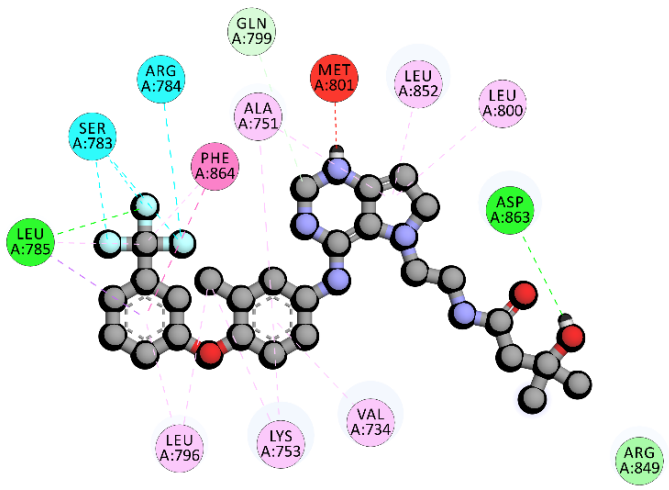
2-isopropyl-2,5-dihydrofuran	

3D Binding Interaction	2D Binding Interaction
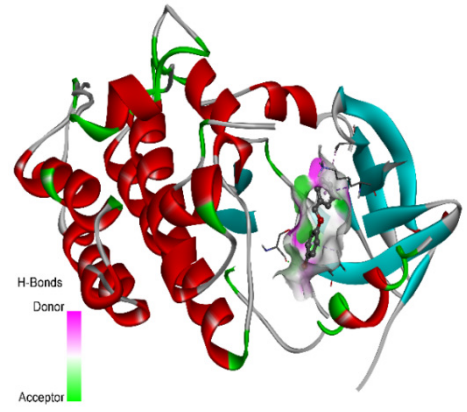	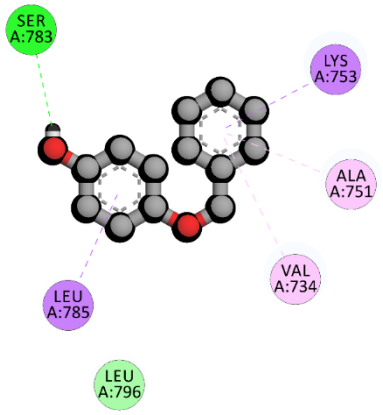
4'-hydroxy-3,6,7-trimethoxyflavone	
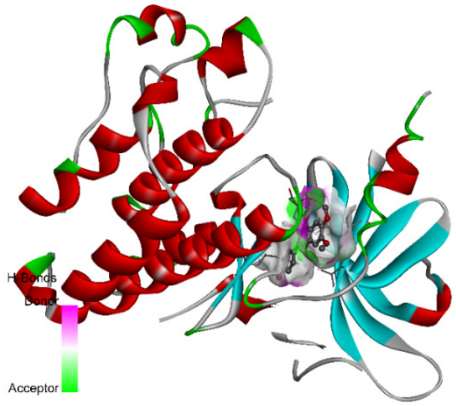	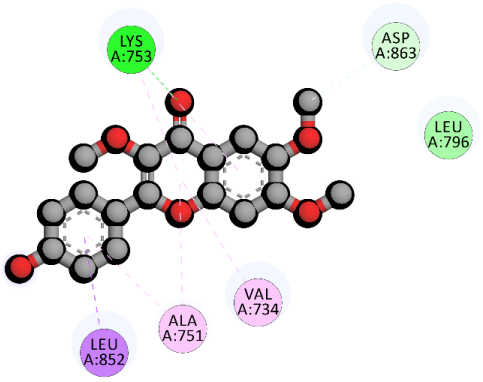
5-hydroxy_2',3,5',6,7-pentamethoxyl_flavone	
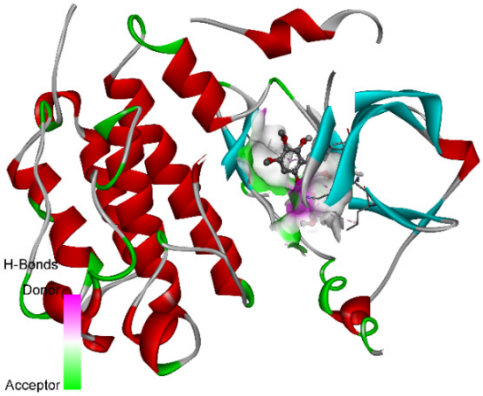	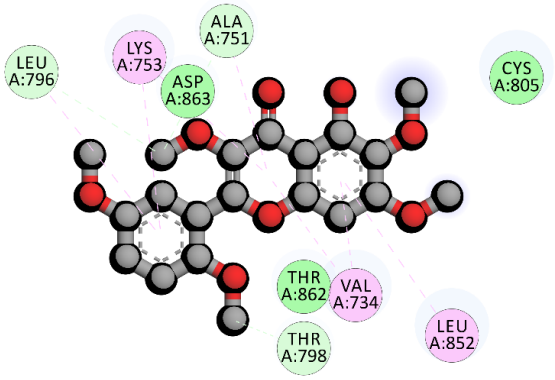
10-methoxy-canthin-6-one	
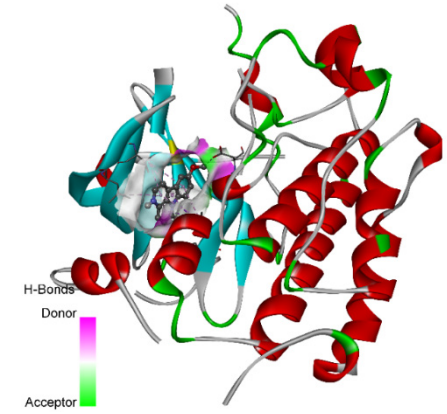	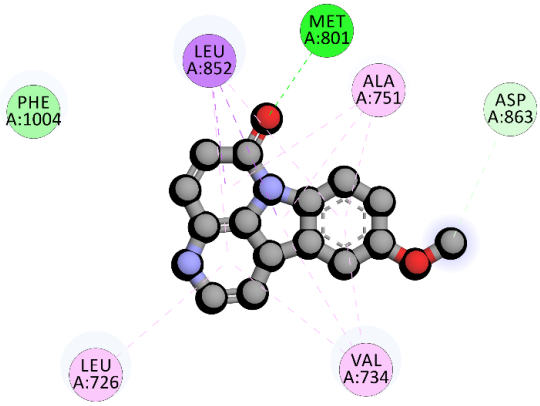

3D Binding Interaction	2D Binding Interaction
Apigenin 7-O-β-D-glucoside	
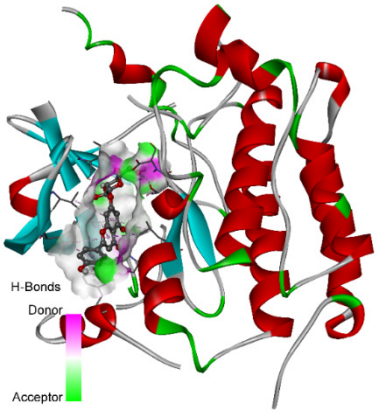	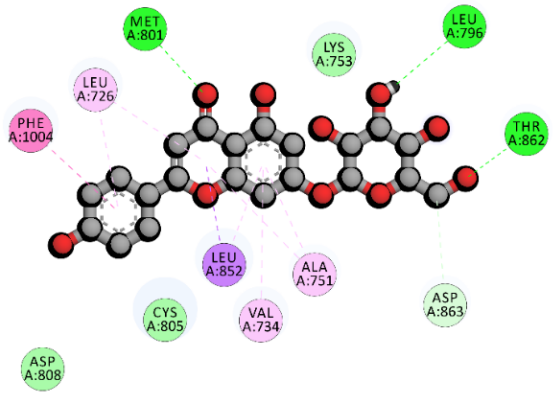
β-carboline-1-propionic acid	
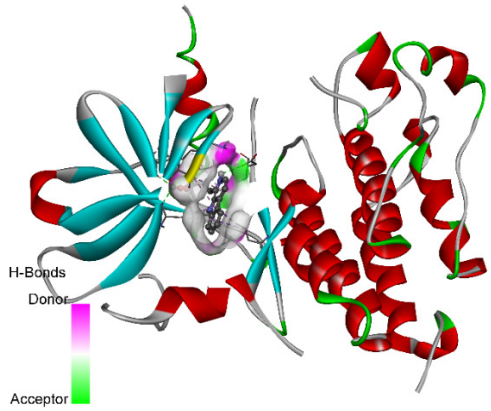	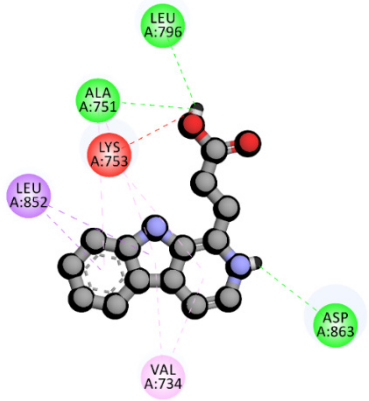
canthin-6-one	
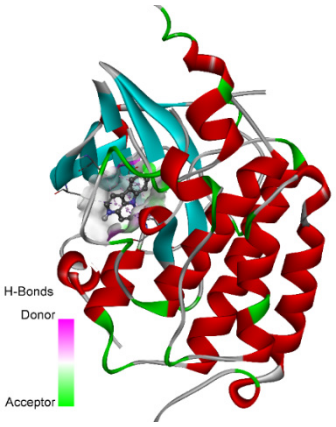	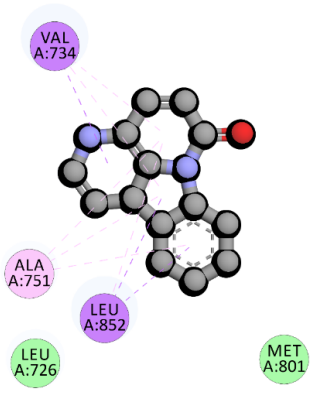
feruloyl_vanillylamine	
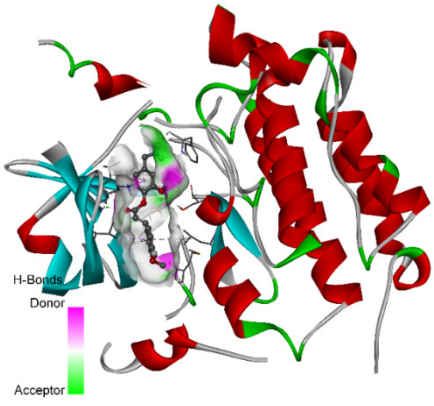	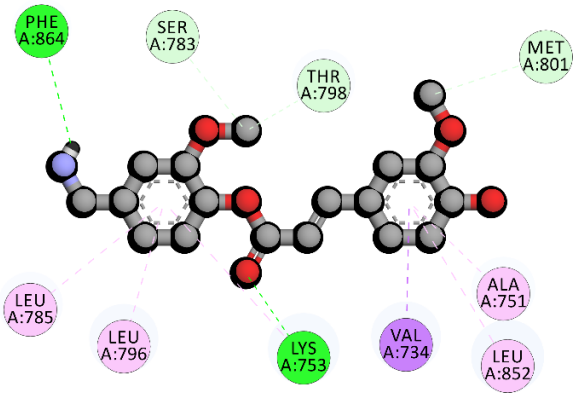

3D Binding Interaction	2D Binding Interaction
Hydroquinone	
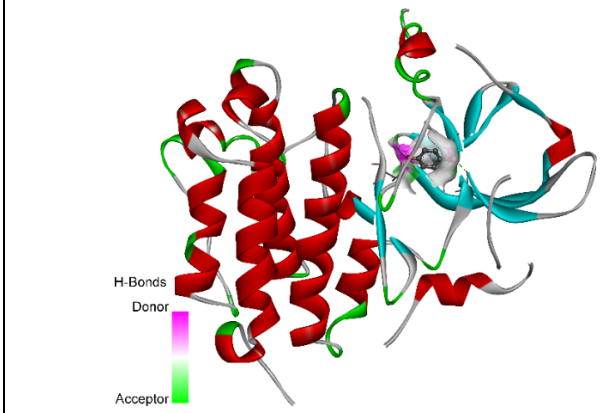	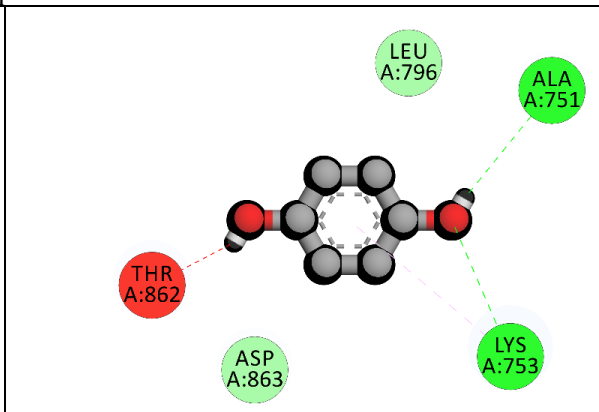
Hydroquinone_monobenzyl	
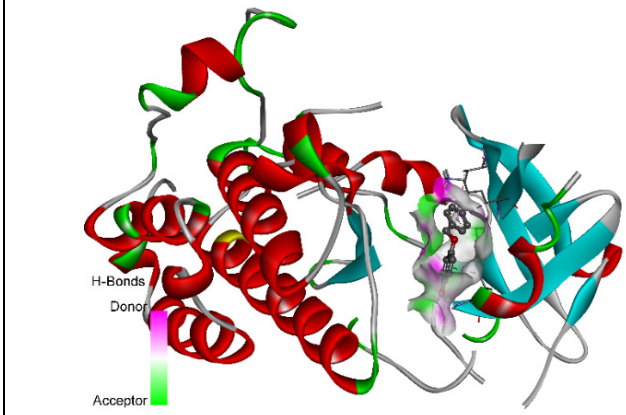	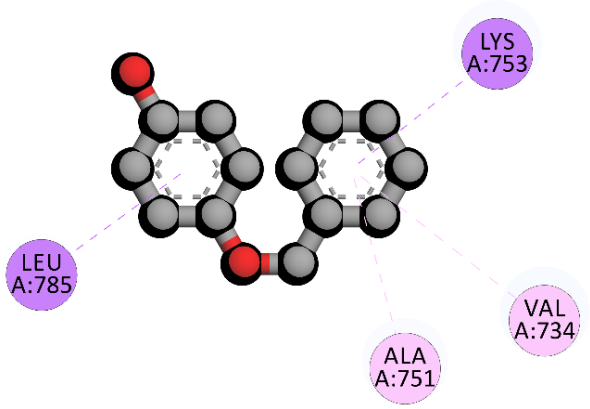
isorhamnetin	
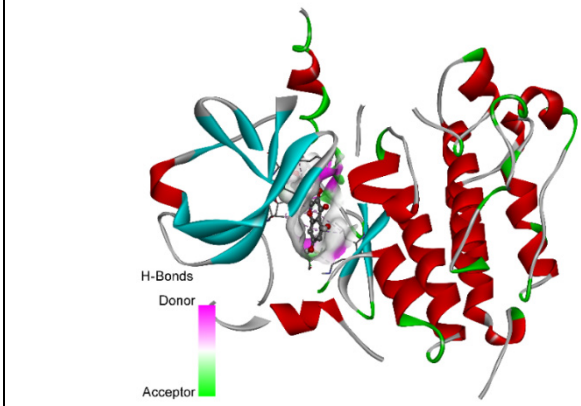	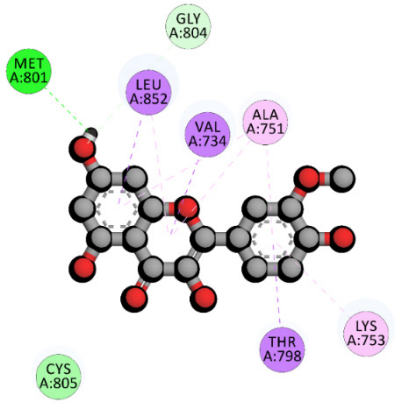
kaempferol	
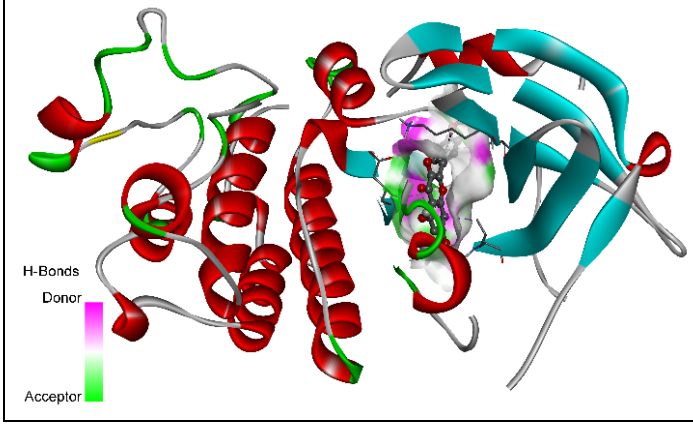	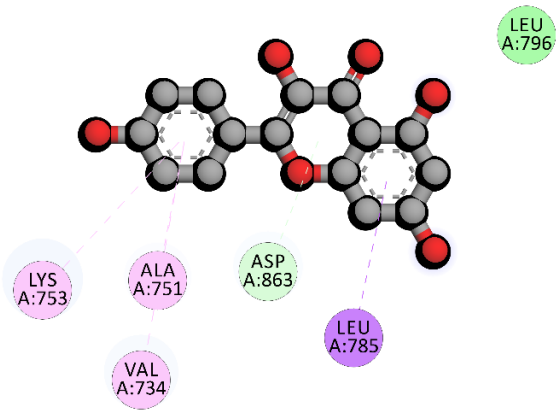

3D Binding Interaction	2D Binding Interaction
p-hydroxy_benzoic_acid	
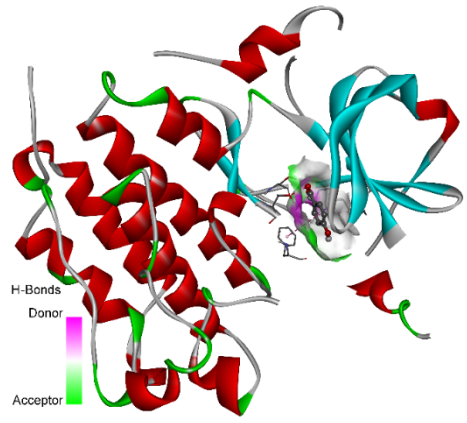	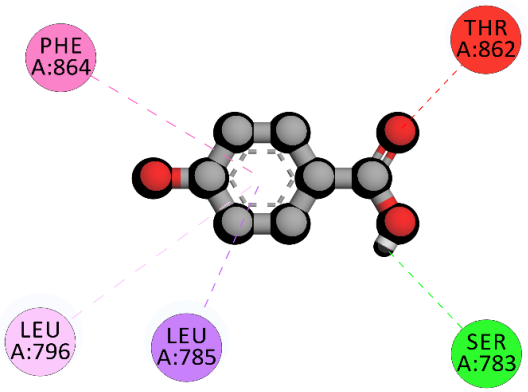
Quercetin	
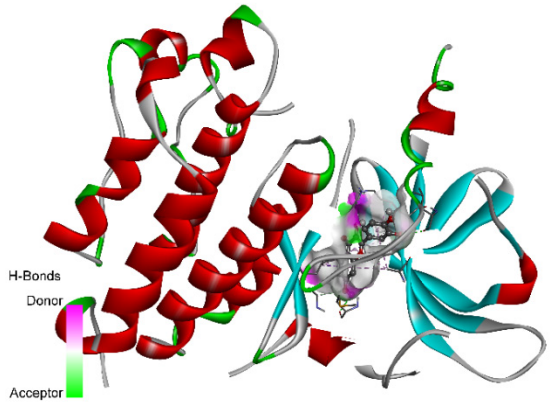	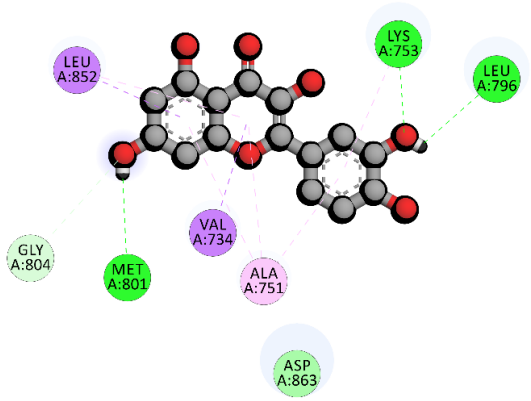
syringic_acid	
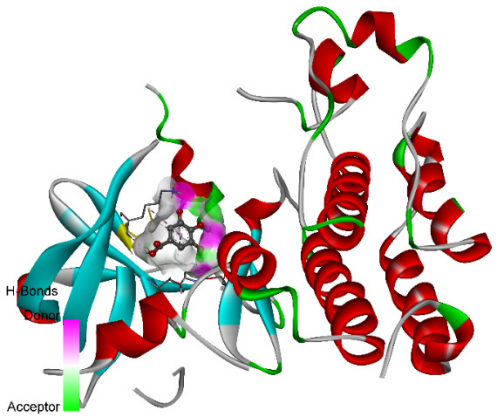	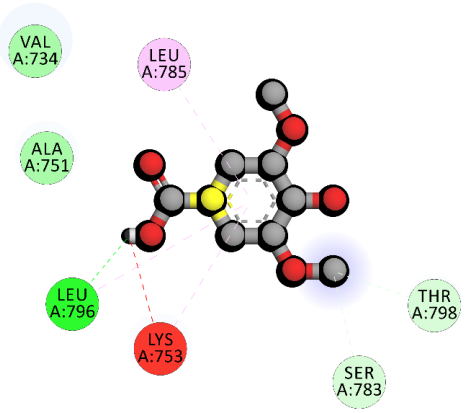
vanillic_acid	
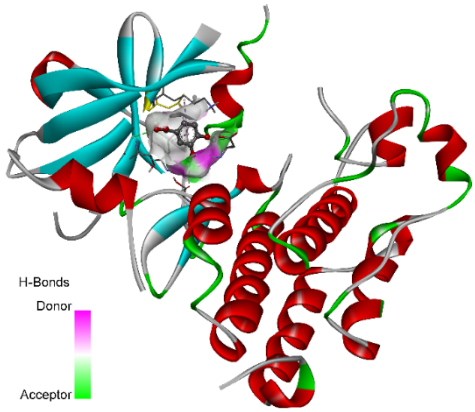	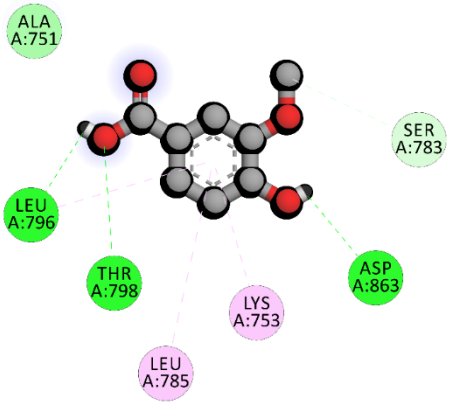

4. Conclusion

This study presents a comprehensive in silico evaluation of phytochemicals from *Aerva lanata* as potential inhibitors of the HER2 kinase, integrating ADMET profiling with molecular docking analysis. The systematic screening of sixteen bioactive compounds highlighted clear structure–activity and pharmacokinetic trends. ADMET assessment revealed that alkaloids and aglycone flavonoids generally possessed favorable physicochemical properties, acceptable absorption profiles, limited toxicity risks, and manageable metabolic liabilities, whereas highly polar glycosylated or low-molecular-weight phenolic acids showed weaker permeability or binding potential. Molecular docking results further strengthened these observations, demonstrating that several phytochemicals exhibited binding affinities comparable to or exceeding that of the native ligand. Notably, apigenin 7-O-β-D-glucoside, 10-methoxy-canthin-6-one, canthin-6-one, and quercetin showed strong docking scores, stable interaction networks, and key hydrogen bonding with critical HER2 active-site residues, indicating robust ligand–protein complementarity.

The combined ADMET–docking workflow effectively prioritized compounds with both pharmacokinetic suitability and strong target engagement. Overall, these findings support *Aerva lanata* as a valuable source of lead scaffolds for HER2-targeted anticancer drug development. The identified candidates warrant further experimental validation through in vitro and in vivo studies to confirm their therapeutic potential and translational relevance.

References

[1] D. C. Joshi, A. Sharma, S. Prasad, K. Singh, M. Kumar, K. Sherawat, et al., Novel therapeutic agents in clinical trials: emerging approaches in cancer therapy (2024).

[2] A. Vikhar, D. Ahmad, M. S. Shaikh and A. S. Tamboli, Luteolin-7-Rutinoside: A Multifaceted Approach to Target Oral Cancer Through Cellular Mechanisms. *J. Pharm. Sci. Comput. Chem.*, 1 (2025) 285–8.

[3] H. S. Samuel, U. D. Akpanke, O. Gideon, E. O. Bulus, M. Fatima and M. I. Matilda, Antioxidant and Phytochemical Classification of Medicinal Plants Used in the Treatment of Cancer Disease. *J. Chem. Lett.*, 5 (2024) 108–19. https://doi.org/10.22034/jchemlett.2024.453132.1179

[4] T. Mukohara, Mechanisms of resistance to anti-human epidermal growth factor receptor 2 agents in breast cancer (2011).

[5] N. Iqbal and N. Iqbal, Human Epidermal Growth Factor Receptor 2 (HER2) in Cancers: Overexpression and Therapeutic Implications. *Mol. Biol. Int.*, 2014 (2014) 1–9. https://doi.org/10.1155/2014/852748

[6] F. Schettini, G. Buono, C. Cardalesi, I. Desideri, S. De Placido and L. Del Mastro, Hormone Receptor/Human Epidermal Growth Factor Receptor 2-positive breast cancer: Where we are now and where we are going (2016).

[7] S. C. Oh, B. H. Sohn, J.-H. Cheong, S. B. Kim, J. E. Lee, K. C. Park, et al., Clinical and genomic landscape of gastric cancer with a mesenchymal phenotype. *Nat. Commun.*, 9 (2018). https://doi.org/10.1038/s41467-018-04179-8

[8] M. A. N. Sendur, S. Aksoy and K. Altundag, Cardiotoxicity of novel HER2-targeted therapies (2013).

[9] D.-B. N. T. Oku, D. D. Babatunde, Y. Nuapia, G. K. More and R. C. Chokwe, Harnessing Machine Learning for the Virtual Screening of Natural Compounds as Both EGFR and HER2 Inhibitors in Colorectal Cancer: A Novel Therapeutic Approach. *ACS Omega* (2025). https://doi.org/10.1021/acsomega.5c07683

[10] N. Govindan, Antioxidant Aerva lanata Extract Supresses Proliferation and Induce Mitochondria Mediated Apoptosis in Human Hepatocelluar carcinoma cell line. *J. Exp. Integr. Med.*, 6 (2016) 71. https://doi.org/10.5455/jeim.270616.or.153

[11] G. Kumar, L. Karthik and K. V. B. Rao, Phytochemical composition and in vitro antioxidant activity of aqueous extract of Aerva lanata (L.) Juss. ex Schult. Stem (Amaranthaceae). *Asian Pac. J. Trop. Med.*, 6 (2013) 180–7. https://doi.org/10.1016/S1995-7645(13)60020-6

[12] T. M. Belete and A. T. Beyna, Review on the Ethnopharmacological Use of Medicinal Plants and Their Anticancer Activity from Preclinical to Clinical Trial (2025).

[13] S. Mani, G. Swargiary, S. Gulati, S. Gupta and D. Jindal, Molecular docking and ADMET studies to predict the anti-breast cancer effect of aloin by targeting estrogen and progesterone receptors. *Mater. Today Proc.*, 80 (2023) 2378–84. https://doi.org/10.1016/j.matpr.2021.06.362

[14] B. M. Amos-tautua, I. T. Ajoko, P. E. Oyaseiye and R. Overe, Computational Screening and ADMET Assessment of Leaf Extracts of Anthocleista djalonensis and Funtumia africana Targeting Tumor Necrosis Factor-Alpha Enzyme. *J. Med. Med. Chem.*, 2 (2026) 43–55. https://doi.org/10.22034/jmedchem.2026.576002.1031

[15] I. A. Ekoro and M. E. Osharode, Computational Insights into Aporphine Alkaloids as Inhibitors of Lassa fever Virus: A Molecular Modelling and DFT Approach. *Med. Med. Chem.*, 2 (2025) 199–223.

[16] M. Goyal, A. Pareek, B. P. Nagori and D. Sasmal, Aerva lanata: A review on phytochemistry and pharmacological aspects. *Pharmacogn. Rev.*, 5 (2011) 195–8. https://doi.org/10.4103/0973-7847.91120

[17] B. Mandal and S. Madan, Aerva lanata: A blessing of Mother Nature. *J. Pharmacogn. Phytochem.*, 5 (2015) 92–101.

[18] A. Shaheen, H. Fida, S. Akhmedov, E. Rasulbek, Z. Ataullaev, In Silico Study of Alkaloids as Potential Cyclin-Dependent Kinase (CDK) Inhibitors. *J. Pharm. Sci. Comput. Chem.*, 1 (2025) 324–35.

[19] P. K. Vawhal, S. B. Jadhav, S. Kaushik, K. C. Panigrahi, C. Nayak, H. Urmee, et al., Coumarin-Based Sulfonamide Derivatives as Potential DPP-IV Inhibitors: Pre-ADME Analysis, Toxicity Profile, Computational Analysis, and In Vitro Enzyme Assay. *Molecules*, 28 (2023). https://doi.org/10.3390/molecules28031004

[20] R. M. Suryawanshi, R. B. Shimpi, V. Muralidharan, L. S. Nemade, S. Gurugubelli, S. Baig, et al., ADME, Toxicity, Molecular Docking, Molecular Dynamics, Glucokinase

activation, DPP-IV, α-amylase, and α-glucosidase Inhibition Assays of Mangiferin and Friedelin for Antidiabetic Potential. *Chem. Biodivers.*, 22 (2025). https://doi.org/10.1002/cbdv.202402738

[21] Q. Siddiqui and Y. A. Shaikh, Hydroalcoholic Extraction of Cissus quadrangularis and In Vitro Evaluation of Antifungal Properties. *J. PharmTechNova*, 01 (2026) 3–10. https://doi.org/10.66220/vyc7rc95

[22] K. Gandla, F. Islam, M. Zehravi, A. Karunakaran, I. Sharma, M. A. Haque, et al., Natural polymers as potential P-glycoprotein inhibitors: Pre-ADMET profile and computational analysis as a proof of concept to fight multidrug resistance in cancer. *Heliyon*, 9 (2023). https://doi.org/10.1016/j.heliyon.2023.e19454

[23] S. A. Ahmed, P. S. Tabassum, S. A. Falak, A. Vikhar, D. Ahmad and S. Shaikh, Molecular Docking and Network Pharmacology: Investigating Vitis vinifera Phytoconstituents as Multi-Target Therapeutic Agents against Breast Cancer. *J. Pharm. Sci. Comput. Chem.*, 1 (2025) 116–34.

[24] F. S. Siddiqui and S. Bhosole, Computational Assessment of Secondary Metabolites as Potential Inhibitors of Methylenetetrahydrofolate Dehydrogenase-2 (MTHFD2). *J. Phytopharm. Adv. Chem.*, 1 (2026) 3–17. https://doi.org/10.66220/wwze8340

[25] A. S. Tamboli and S. D. Tayade, In-Depth Investigation of Berberine and Tropane through Computational Screening as Possible DPP-IV inhibitors for the Treatment of T2DM. *J. Pharm. Sci. Comput. Chem.*, 1 (2025) 1–11.

[26] B. M. Amos-tautua, I. T. Ajoko, S. O. Ibrahim, In Vitro and In Silico Evaluation of ADME / Drug-Likeness and Docking Studies of Bioactive Carotenoids from Capsicum chinense with Antioxidant Potential. *Chem. Res. Technol.*, 3 (2026) 1–22.

[27] F. A. Siddiqui, R. Makhloufi, M. Hojjati, M. S. El-sayed, K. Eman, Computational Exploration of Quinine and Mefloquine as Potential Anti-Malarial Agents. *J. Pharm. Sci. Comput. Chem.*, 1 (2025) 106–15.

[28] M. A. Abubaker, K. W. Omari, Z. A. Baki, P. R. Shakya, H. M. A. Hasan, S. M. Saleh, et al., Computational Evaluation of Cryptolepine and Tryptanthrin as Potential α-Glucosidase Inhibitors. *J. Pharm. Sci. Comput. Chem.*, 1 (2025) 336–46.

[29] D. Roy, Drug repurposing of some US FDA-approved drugs using Binding strength Studies for the Treatment of Methicillin-resistant Staphylococcus aureus Infection. *J. Phytopharm. Adv. Chem.*, 1 (2026) 30–44.

[30] S. N. Adawara, A. S. Isa, F. A. Yaro, A. Tijjani Mustapha, U. T. Mamza, M. Iji, et al., Triazolopyrimidine Derivatives for Cancer: An In Silico Evaluation of Docking and Pharmacokinetics. *J. Chem. Technol.*, 1 (2025) 116–25.